EPJ manuscript No.
(will be inserted by the editor)

Control of Optical Dynamic Memory Capacity of an Atomic Bose-Einstein Condensate

Devrim Tarhan[1], Alphan Sennaroglu[2], and Özgür E. Müstecaplıoğlu[2]

[1] Harran University, Department of Physics, 63300 Osmanbey Yerleşkesi, Şanlıurfa, Turkey
[2] Koç University, Department of Physics, Rumelifeneri Yolu, 34450 Sarıyer, Istanbul, Turkey

Abstract. Light storage in an atomic Bose-Einstein condensate is one of the most practical usage of these coherent atom-optical systems. In order to make them even more practical, it is necessary to enhance our ability to inject multiple pulses into the condensate. In this paper, we report that dispersion of pulses injected into the condensate can be compensated by optical nonlinearity. In addition, we will present a brief review of our earlier results in which enhancement of light storage capacity is accomplished by utilizing multi-mode light propagation or choosing an optimal set of experimental parameters.

1 Introduction

Soon after the generation of Bose Einstein condensate in an ultracold gas of trapped Alkali atoms [1], a promising utilization of it for the dramatic slowing down of a light pulse was demonstrated [2]. This feat is accomplished with the help of a quantum coherent effect called electromagnetically induced transparency (EIT) [3,4]. Ultraslow light pulses can be used for storage of coherent optical information [5]. Mutual conversion of classical coherent information (phase and amplitude) of the light pulse and the quantum information (quantum state) of the atomic system can allow for quantum information processing via ultraslow light [6]. A quite recent experiment provides strong hope towards this direction [7]. In the experiment, coherent optical information is first encoded in one condensate. Quantum information in the condensate is then carried to another condensate by a matter wave. Finally, coherent optical information is revived in an optical pulse, generated out of the new condensate on demand.

Due to such impressive developments in experimental ability to control of light and matter waves in light storage experiments, more practical quantum information processing applications can be expected to occur in near future. On the other hand, it is necessary first of all, to increase our capability to control the amount of information stored in the condensate. For that aim, we should be able to inject more than one pulse into the condensate during the storage time. This is a basic requirement to realize practical logic gates in atomic condensates using slow light set ups [5,6].

To investigate how to make more than one pulse simultaneously present in an atomic condensate efficiently, we have performed a series of studies. This paper reviews some of our earlier results and in addition it reports our new results where we have found optimum conditions for dispersion compensation via nonlinearity. In our earlier works, we show that optical dynamic memory capacity of the condensate can be optimized by choosing a certain set of experimental control parameters, such as coupling laser Rabi frequency and temporal width of the probe pulse for a given atomic condensate [8]. It has been shown that axial density profile of the condensate helps to preserve the probe pulse shape against group velocity dispersion [8]. Further enhancement of the memory capacity can be possible by taking into account radial confinement of the probe pulse. We have demonstrated that a particular radial density profile of the condensate reduces the effect of modal dispersion and contributes to the pulse shape preservation [9]. We deduce that the optical control parameters are beneficial for optimizing the memory capacity and at the same time, properties of the atomic cloud can also be exploited to enhance the maximum capacity available. When we take into account radial confinement, ultraslow wave-guiding regimes have been investigated and characterized. Propagation constants and the conditions on the number of ultraslow optical modes have been determined. Detailed numerical examinations revealed the ultraslow mode profiles that can be supported by atomic condensates. In this paper, we will go beyond these linear optical results and examine the effects of nonlinear optical response of the condensate. We show that ultraslow solitons can bring further enhancement in the light storage capacity.

Following this introduction, in Sec. 1, the paper first reviews optical information storage enhancement schemes based upon linear optics considerations. In Sec. 2.1., group velocity dispersion and a scheme to beat it are discussed. In Sec. 2.2, taking into account transverse directions to the propagation direction, modal dispersion is studied. Information storage enhancement with the aid of ultraslow waveguiding modes are discussed. Our new contributions in which ultraslow light propagation is studied in the nonlinear regime is described in Sec. 3. Increase in the capacity of optical information storage due to the ultraslow optical solitons is discussed in that section. Finally, we conclude in Sec. 4.

2 Control of optical information storage in linear optical regime

To slow down group velocity of an optical pulse just to few meter per second, steep dispersion of electromagnetically induced transparency is used [2]. Optical pulse to be slowed down consists of a weak probe light. It is shined upon atomic BEC, together with a stronger control field. This configuration allows for cancellation of absorption at resonance and creates transparency over a small frequency window. Measuring the axial length of the condensed cloud by an imaging laser and comparing the time delay in the probe beam propagation with a reference beam not entered into the condensate determines operationally the average group speed of the probe pulse. Such a typical slow light experiment is usually modelled by a one dimensional linear optics model. This model predicts the measured group speeds well, especially when the interactions within the cloud is taken into account [10].

Considering a gas of effectively three-level atoms, linear optical response of an EIT medium is characterized by a susceptibility given by

$$\chi = \frac{\rho|\mu_{31}|^2}{\epsilon_0\hbar}\frac{i(i\Delta+\Gamma_2/2)}{[(\Gamma_2/2+i\Delta)(\Gamma_3/2+i\Delta)+\Omega_c^2/4]}. \tag{1}$$

The effective level configuration of the atoms consists of two dipole allowed transitions such that the lower levels $|1\rangle$ and $|2\rangle$ are coupled to the upper level $|3\rangle$ by the probe and the control fields, respectively. Here, ρ is atomic (number) density. We assume that the control field of Rabi frequency Ω_c is at resonance, while Δ is the detuning of the probe field of frequency ω from the resonance frequency ω_0. μ_{31} is the dipole matrix element for the probe transition. Taking resonance wavelength λ for the probe transition we have the usual relation $\mu_{31}^2 = 3\epsilon_0\hbar\lambda^3\gamma/8\pi^2$ with γ is the spontaneous decay rate for the probe transition. Dephasing rates of the corresponding transitions are denoted by Γ_2 and Γ_3. Within a small frequency window about the probe resonance, susceptibility becomes a negligibly small pure imaginary number, which leads to the transparency effect. Besides, within this window, susceptibility shows steep variation with Δ so that group velocity reduces dramatically for a resonant probe pulse that can propagate without suffering any significant absorption. Physically, this is possible by the cancellation of absorption due to the destructive quantum interference of the transition probabilities to the upper level. Quantum coherence is established by the control field which is stronger than the probe field in the usual EIT condition.

It may be argued that BEC is not essential for the ultraslow light generation. Degenerate Fermi gas also allows for significant reduction in group velocity, though not as efficient as BEC [11]. BEC gives much slower speeds over more compact spatial dimensions. Its unique advantage however is the ability to combine matter wave dynamics with the ultraslow light pulses [7]. This seems to be more promising for practical quantum information processing.

Susceptibility formula is derived by the steady state solution of the Liouville equation for the density matrix, assuming most of the atoms remain in level $|1\rangle$. In the subsequent section, we will go beyond linear regime and consider nonlinear response. In the linear regime, we will first discuss dispersive propagation of ultraslow short pulses in one dimension. After that, we extend this by taking into account transverse directions as well.

Dispersive effects are weak in the usual ultraslow light experiments as these pulses are just a few microseconds long. First attempts to model experimental system uses one dimensional non-interacting BEC as the propagating medium with linear optical response [12]. Furthermore it is assumed that the medium is non-dispersive. This model is improved significantly by considering atom-atom interactions. It has been shown that increasing interactions lead to faster group speeds [10]. Higher dimensional propagation effects within paraxial approximation are also considered and diffraction effects at the thermal cloud boundary of the condensate are numerically simulated [10]. These results demonstrate validity of the non-dispersive, one-dimensional model in describing experimental results. On the other hand, when it comes to improve storage capacity, this model becomes insufficient.

Natural attempt to enhance our ability to inject multiple pulses into the BEC during the storage time is to use shorter pulses in time. By this way, if we say every pulse carries a bit of coherent optical information (which is the classical information associated with the amplitude and phase of the pulse), then we could achive higher bit storage capacity. With the usual microsecond pulses however, as the storage time is also about a few microseconds, one can get only one pulse present in the condensate [2]. Some schemes are proposed to increase number of pulses. One can utilize for instance different polarization of probe pulses [13] or enhancement of EIT window [14]. Both these proposals would benefit from more direct approach of being able to inject shorter pulses into the condensate [15,16,17]. The fundamental problem in using shorter pulses is that they may be broadened due to the group velocity dispersion within the storage time. It is thus necessary to study effect of group velocity dispersion in the axial propagation of ultraslow short pulses in order to estimate actual enhancement of the bit storage capacity.

2.1 Group velocity dispersion

We will now investigate the propagation of short laser pulses under slowly varying phase and envelope approximations without taking into account nonlinear optical response. A formulation of light propagation through a dispersive EIT medium is given in Ref. [18]. We have applied this theory to ultraslow short light pulses through BEC in Ref. [8]. We now review and summarize our major results in Ref. [8].

Total polarization is related to the electric field through electric susceptibility via $\mathbf{P} = \mathbf{P^{(1)}}$ where the linear polarization is $\mathbf{P^{(1)}} = \epsilon_0\chi(\omega)^{(1)}\mathbf{E}$. Dispersive medium is characterized by a frequency dependent susceptibility. We write $P(\omega-\omega_0, E) = \epsilon_0\chi(\omega-\omega_0)^{(1)}E(\omega-\omega_0)$. Expanding the linear susceptibility $\chi^{(1)}$ of the dressed atom to second order about a central frequency ω_0,[18]

$$\chi(\omega-\omega_0)^{(1)} = \chi(\omega_0) + \frac{\partial\chi}{\partial\omega}|_{\omega_0}(\omega-\omega_0) + \frac{1}{2}\frac{\partial^2\chi}{\partial^2\omega}|_{\omega_0}(\omega-\omega_0)^2, \tag{2}$$

polarization becomes

$$P(t) = \epsilon_0\chi(\omega_0)^{(1)}E(t) - i\epsilon_0\frac{\partial\chi^{(1)}}{\partial\omega}|_{\omega_0}\frac{\partial E}{\partial t} - \frac{\epsilon_0}{2}\frac{\partial^2\chi^{(1)}}{\partial^2\omega}|_{\omega_0}\frac{\partial^2 E}{\partial^2 t}. \tag{3}$$

In slowly varying approximation, the wave-equation is given by,

$$\frac{\partial E}{\partial z} + \frac{1}{c}\frac{\partial E}{\partial t} = \frac{ik}{2\varepsilon_0}P. \tag{4}$$

Using equation (3) in Eq. 4, we obtain the wave equation for the short optical pulse such that

$$\frac{\partial E}{\partial z} + \alpha E + \frac{1}{v_g}\frac{\partial E}{\partial t} + i\, b_2 \frac{\partial^2 E}{\partial t^2}, \tag{5}$$

where α determines the pulse attenuation; v_g is the group velocity, b_2 is the second-order dispersion coefficient, or the group velocity dispersion. Calculating the third and the second order dispersion coefficients using typical experimental parameters [2] but for shorter pulses, we have found that third order dispersion is seven orders of magnitude smaller and negligible. Second order dispersion becomes significant for pulses shorter than microseconds. In our numerical calculations, we consider parameters for the experiment in Ref. [2] except for the coupling field Rabi frequency which is chosen to be $\Omega_c = 5\gamma$. The transmission window, $\Delta\omega$ is calculated to be $\Delta\omega = 8.49 \times 10^7$ Hz so that we shall consider pulses of width up to $\tau = 10$ ns for efficient transmission. The coefficients can be calculated directly from the susceptibility via

$$\alpha = -\frac{i\pi}{\lambda}\chi(\omega_0), \tag{6}$$

$$\frac{1}{v_g} = \frac{1}{c} - \frac{\pi}{\lambda}\frac{\partial \chi}{\partial \omega}|_{\omega_0}, \tag{7}$$

$$b_2 = \frac{\pi}{2\lambda}\frac{\partial^2 \chi}{\partial \omega^2}|_{\omega_0}. \tag{8}$$

These expressions lead to complex parameters in general, as χ is a complex valued function. At EIT resonance, they lead to physically meaningful well-defined real valued absorption coefficient, group velocity and dispersion coefficient. When Rabi frequency for the coupling field is sufficiently large such that $\Omega_c \gg \Gamma_{2,3}$, the coefficients reduce to

$$\alpha = \frac{2\pi\rho|\mu_{31}|^2\Gamma_2}{\epsilon_0\hbar\lambda\Omega_c^2}, \tag{9}$$

$$v_g = \frac{c\epsilon_0\hbar\Omega_c^2}{2\omega_{31}|\mu_{31}|^2\rho}, \tag{10}$$

$$b_2 = i\frac{8\pi\Gamma_3|\mu_{31}|^2\rho}{\epsilon_0\hbar\lambda\Omega_c^4}. \tag{11}$$

$$\tag{12}$$

It should be noted that the given expression for for v_g is valid only when

$$\Gamma_{2,3} \ll \Omega_c \ll \sqrt{4\pi c|\mu_{31}|^2\rho/\epsilon_0\hbar} = \sqrt{\frac{3}{4\pi}c\lambda^3\gamma\rho}. \tag{13}$$

From the explicit expressions, we see that v_g increases more slowly with the Rabi frequency of the control field Ω_c than the decrease of the dispersion coefficient b_2. This higher susceptibility of b_2 to Ω_c can be exploited to optimize the bit storage capacity C, defined by $C = L/2v_g\tau$ with τ is the largest width of the probe pulse within the condensate of size L.

Analytical solutions for C are derived for a Gaussian pulse assuming a uniform effective dispersive medium representing the actual spatially inhomogeneous BEC [8]. Analytical solution of the wave equation allows for determination of the pulse width. L is calculated as the root-mean-square of the axial distance for a given condensate of number density ρ, under a semi-ideal model of the weakly interacting condensate [19]. This leads to

$$C = \frac{L}{2\tau_0\sqrt{4\pi^2\Omega_c^4/9\lambda^4\gamma^2\rho^2 + 4L^2\Gamma_3^2/\pi^2\tau_0^4\Omega_c^4}}. \tag{14}$$

Initial pulse width is denoted by τ_0. C shows a maximum at a critical Rabi frequency determined by

$$\Omega_{c0} = \left(\frac{3\Gamma_3\lambda^2\gamma\rho L}{\pi^2\tau_0^2}\right)^{1/4}. \tag{15}$$

The corresponding storage time of the pulse t_{s0} is given by

$$t_{s0} = \tau_0 \left(\frac{\sqrt{3}\lambda\sqrt{\gamma}}{2\sqrt{\Gamma_3}} \right) \left(\sqrt{\rho L} \right). \tag{16}$$

From the number of pulses that can be present in this storage time we find the maximum capacity as,

$$C_{max} = \sqrt{\frac{3\gamma\lambda^2 L\rho}{32\Gamma_3}}, \tag{17}$$

which is independent of the pulse width at the critical Rabi frequency. At the critical Rabi frequency, about two orders of magnitude improvement is achieved regarding the bit storage capacity.

More rigorous numerical calculations are verified these analytical results. Numerical calculations take into account density variations and the thermal component of the gaseous system. Temperature and the interactions affect the pulse character through the dependence of pulse parameters on spatial size and density product. Numerical studies are required to handle spatially inhomogeneous BEC. Propagation parameters in the wave equation gain non-local character under this model but can be treated numerically. We have found that as the pulse gets broader and broader as it propagates towards to the central region of the atomic cloud, where the dispersive effects are most strong, it becomes better protected against dispersion. As it is already broadened, it gets less broadening effect. Axial density profile of the condensate protects the pulse against group velocity dispersion. Thermal variation of the bit storage capacity is investigated numerically and just below critical temperature, an optimum temperature for the highest capacity is determined. Interactions in the cloud effects the broadening of the pulse and makes it more sharp when the interactions are stronger. Fig. 1 illustrates these results.

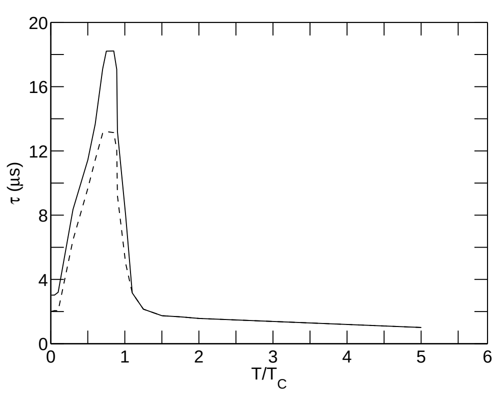

Fig. 1. Temperature dependence of the pulse width calculated numerically for an inhomogeneous condensate profile. Initial width of the pulse is 1 ns. Effect of the interactions can be seen by comparing the solid curve for which the s-wave scattering length characterizing the effective atom-atom interactions $a_s = 2.75$ nm with the dashed one for which $a_s = 7$ nm. The parameters used in the calculation are taken from the experiment in Ref. [2].

From the figure we see that the short pulses suffer significant broadening despite the short size of the condensate. One cannot increase the capacity C thousand times by using nanosecond pulses instead of microsecond ones. Using a control field at the suggested critical value as above, an optimum increase of the number of pulses that can be injected multiply into the condensate can be achieved. Analytical result of C evaluated gives about 80 pulses in the condensate while numerical result suggests, as explained above, due to less broadening within the inhomogeneous condensate, 800 pulses could in fact be stored. In comparison to present slow light experiments, that means a two orders of magnitude enhancement in the bit storage capacity. Below we shall discuss additional improvements to C, taking into account transverse directions of the condensate as well as nonlinearity in the probe pulse propagation.

2.2 Modal dispersion

In a subsequent analysis we take into account transverse dimensions to the axial propagation direction and examine the ultraslow optical modes. Waveguiding problems in cold gaseous systems was subject to much attention recently [20,21,22,23]. Now we summarize our major results reported in Ref. [9]. We observe that at extremely low temperatures well below the critical temperature of condensation, density profile of the condensate can be approximately described by Thomas-Fermi approximation. Normally, at perfect EIT resonance, no significant index difference between the condensate core and the thermal background gas can be achieved. In this case, only single mode is supported in the condensate. For a slightly off-resonant probe however, sufficiently high index contrast can be generated between the condensed core and the enveloping thermal gas. Under these conditions, radial density of the condensate can be translated to a graded index profile characterized by a parabolic (quadratic) spatial variation in the form

$$n(r) = \begin{cases} n_1[1 - A(\frac{r}{R})^2]^{1/2} & r \leq R. \\ 1 & r \geq R \end{cases} , \tag{18}$$

with $A = 1 - 1/n_1^2$. Here R is the thermal radius along the transverse (radial, r) direction and n_1 is the index along the axial (z) direction. Such a system resembles a graded index fiber, though one of micron sized. Light propagation is found to be in the weakly guided regime where the optical modes are described in terms of linearly polarized (LP) modes as the index difference is small and the axial component of the electric field is negligible. In this case the radial wave equation is described by the Helmholtz radial equation

$$\left[\frac{\mathrm{d}^2}{\mathrm{d}r^2} + \frac{1}{r}\frac{\mathrm{d}}{\mathrm{d}r} + k_0^2 n^2(r) - \beta^2 - l^2/r^2\right]\psi(r) = 0. \tag{19}$$

Here $k_0 = \omega/c, l = 0, 1, 2, ..., \beta$, and ψ are defined for the transverse field of the LP modes $E_t = \psi(r)\exp\left[\mathrm{i}(l\phi + \omega t - \beta z))\right]$.

The number of such transverse (LP) modes as well as their group velocity is evaluated. We find that modal dispersion is stronger at low temperatures and large number of modes can be supported by the condensate. As the temperature gets higher and higher, number of modes that can be supported decrease. This is due to the shrinkage of the condensate and the vanishing of the index contrast. Analytical results are provided by a conventional WKB treatment. Conditions for multiple, single and two mode propagations are provided. It is shown that all LP modes can propagate at ultraslow light speeds. Lower order modes propagate slower while higher order modes goes faster as they are away from the central, more dense, condensed region. This particular density profile of the BEC then allows for less pulse spread due to differences in the group speeds of different modes. As in the case of axial propagation where axial density of the condensate protects the pulse against group velocity dispersion, now the radial profile of the condensate also helps for the pulse shape preservation against modal (waveguide) dispersion. More detailed numerical studies are performed. We consider the condensate in terms of tiny shells and treat the index as constant within each region between the shells. At constant index, analytical solutions in terms of Bessel function are written down and matched at the boundaries. By this way, actual mode profiles are numerically determined. We illustrate two modes in Fig. 2.

Short axial size of BEC and its unique density profile can be exploited to keep modal dispersion weak. In such short distance applications, this may be utilized to capture optimum amount of power from a light source and enhance the optical coupling/sensing capability of BEC.

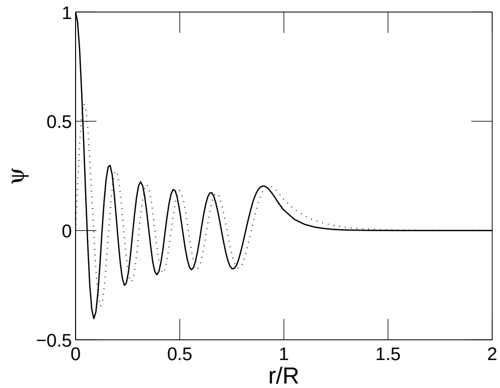

Fig. 2. Two ultraslow transverse modes confined in a BEC. Solid curve is for LP_{00} while the dotted one is for LP_{10}. Mode profiles are calculated with the parameters that are taken from the experiment in Ref. [2], except for $\Delta = -0.1\gamma$ and $\Omega_c = 2.5\gamma$.

LP modes can be addressed by specifically constructed transverse profiles of the probe pulses. This can be exploited to control of capacity in the transverse direction for storage of coherent optical information in different mode patterns. These results can be further combined with the longitudinal control of optical information storage capacity where a particular EIT scheme, in which the control field is perpendicular to the probe field, is employed [24].

3 Control of optical information storage in nonlinear optical regime

We will now take into account nonlinear optical response of the condensate in the short pulse propagation. Total polarization, now including the contribution of nonlinear polarization $\mathbf{P^{(nl)}} = \epsilon_0(\chi(\omega)^{(2)} : \mathbf{EE} + \chi(\omega)^{(3)} : \mathbf{EEE})$, can be expressed as

$$P(\omega-\omega_0, E) = \epsilon_0\chi(\omega-\omega_0)^{(1)}E(\omega-\omega_0) + \epsilon_0\chi^{(2)} : \mathbf{EE} + \epsilon_0\chi^{(3)} : \mathbf{EEE}, \tag{20}$$

where an expression for the third order nonlinear susceptibility is given in Ref. [25]. This introduces nonlinear terms to the susceptibility expansion so that polarization can be written as

$$\begin{aligned} P(t) = \epsilon_0\chi(\omega_0)^{(1)}E(t) - i\epsilon_0\frac{\partial\chi^{(1)}}{\partial\omega}|_{\omega_0}\frac{\partial E}{\partial t} - \frac{\epsilon_0}{2}\frac{\partial^2\chi^{(1)}}{\partial^2\omega}|_{\omega_0}\frac{\partial^2 E}{\partial^2 t} \\ + \epsilon_0\chi^{(2)} : \mathbf{EE} + \epsilon_0\chi^{(3)} : \mathbf{EEE}. \end{aligned} \tag{21}$$

$\chi^{(2)}$ is zero due to the inversion symmetry of BEC. Using Eq. (21) in Eq. (4), we get a nonlinear wave equation for the short optical pulse such that

$$\frac{\partial E}{\partial z} + \alpha E + \frac{1}{v_g}\frac{\partial E}{\partial t} + i\,b_2\frac{\partial^2 E}{\partial t^2} + i\eta|E|^2E = 0, \tag{22}$$

where η is the nonlinear optical Kerr coefficient that can be calculated from the susceptibility via

$$\eta = -\frac{\pi}{\lambda}\chi^{(3)}(\omega_0). \tag{23}$$

When $\Omega_c \gg \Gamma_{2,3}$, we find

$$\eta = \frac{4\pi\rho|\mu_{31}|^4\Gamma_2}{3\varepsilon_0\hbar^3\lambda\Gamma_3}\frac{(\Gamma_2+\Gamma_3)}{\Omega_c^4} \tag{24}$$

Let us now write the wave equation (22) in a more conventional form [26],

$$\frac{\partial E}{\partial z}+\frac{\alpha^{'}}{2}E+\beta_1\frac{\partial E}{\partial t}+\frac{i}{2}\beta_2\frac{\partial^2 E}{\partial t^2}+i\eta|E|^2E=0. \tag{25}$$

Here $\beta_1=1/v_g$, $\beta_2=2b_2$ and $\alpha^{'}=2\alpha$. By making transformation $T=t-z/v_g$, $A=\sqrt{\epsilon_0 c}E$ and $\gamma=\eta/\epsilon_0 c$ [26] we obtain

$$i\frac{\partial A}{\partial z}+i\frac{\alpha^{'}}{2}A-\frac{1}{2}\beta_2\frac{\partial^2 A}{\partial T^2}-\gamma|A|^2A=0. \tag{26}$$

where A is the slowly varying amplitude of the pulse envelope.

Spatial variation of the nonlinear optical Kerr coefficient in the axial direction is shown in Fig. (3). Fig. (4) displays the axial spatial profile of the second-order dispersion coefficient. These figures demonstrate a potential for compensation of the dispersion by nonlinearity is

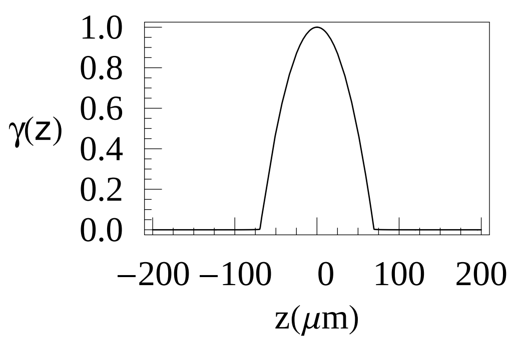

Fig. 3. Axial spatial profile of the nonlinear coefficient γ for the parameters same with those of Fig.1. γ is normalized by its peak value 3.64×10^{-6} m/W.

possible. We need to determine required laser power for that aim.

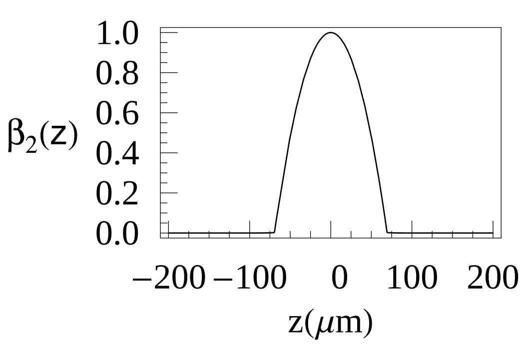

Fig. 4. Axial spatial profile of the second-order dispersion coefficient β_2 for the parameters same with those of Fig.1. β_2 is normalized by its peak value 1.07×10^{-11} s^2/m.

In order to solve Eq. (26) one can introduce normalized amplitude U by using the definition [26]

$$A(z,\tau)=\sqrt{P_0}exp(-\alpha^{'}z/2)U(z,\tau). \tag{27}$$

where P_0 is the peak intensity of the incident pulse and $\tau=T/T_0$ with initial pulse width T_0. The dispersion length L_D and the nonlinear length L_{NL} provide length scales over which dispersive or nonlinear effects become important for the pulse evolution in the Bose-Einstein condensate with an effective length L. The dispersion length L_D and the nonlinear length L_{NL} are given by [26]

$$L_D = \frac{T_0^2}{|\beta_2|}, \tag{28}$$

$$L_{NL} = \frac{1}{\gamma P_0}. \tag{29}$$

For the nonlinear pulse propagation, a dimensionless parameter N is introduced as

$$N^2 = \frac{L_D}{L_{NL}} = \frac{\gamma P_0 T_0^2}{|\beta_2|}. \tag{30}$$

For values $N \approx 1$ both Self-phase modulation(SPM) and Group-velocity dispersion(GVD) play an equal role [26]. Under this condition, we determine the peak power to compensate the group-velocity dispersion for a short optical pulse propagating in the BEC using

$$P_0 = \frac{|\beta_2|}{T_0^2 \gamma}. \tag{31}$$

Using Eqs. (11) and (24), we find the relation between the probe pulse characteristics and the material parameters such that

$$P_0 T_0^2 = \frac{32\pi^2 \hbar c}{\lambda^3} \frac{\Gamma_3}{\gamma \Gamma_2}. \tag{32}$$

Using the parameters given in the slow light experiment Ref.[2], such that $\gamma/2\pi = 10.01$ MHz, $\lambda = 589.76$ nm, $\Gamma_3 = \gamma/2$, $\Gamma_2/2\pi = 1$ kHz, we calculate that $P_0 = 389$ mW/cm^2 for a 1 μs pulse. For a shorter pulse of 10 ns, required intensity increases to 3.9 kW//cm^2. These intensities are beyond the saturation intensity of the corresponding transition for the sodium atom, which is in the order of ~ 10 mW/cm^2. However, it is common to consider high intensities, in particular for the control field in EIT. For example, Ref. [25] considers a control field of intensity 55 mW/cm^2. In the EIT process, absorption of the probe field is cancelled due to the quantum interference of the transition amplitudes. The major limitation on the probe intensity is the EIT condition itself, which requires much higher control field Rabi frequencies than that of the probe field. If we use the same parameters with Ref. [25], which takes slightly different decoherence and decay rates than the ones used in the experiment in Ref. [2], we would get $P_0 = 1.6$ mW/cm^2 for a 1 μs pulse and $P_0 = 166$ mW/cm^2 for a 0.1 μs pulse. Sensitivity of the required peak intensity on the natural linewidths and the decoherence rate of the atomic system suggest that one can engineer linewidths using different atoms, level structures [30] and putting the atoms in an optical cavity [31] to optimize demanded peak intensity. Furthermore, instead of a continuous wave (cw) shining upon the condensate, we consider storage of pulse trains inside the condensate, and hence the average power would be smaller than the one associated with the peak intensity. The results reported here can be extended to the ultraslow pulses in hot gases as well, by taking into account Doppler and collision broadenings. In such systems, much higher pulse intensities in the orders of $1 - 1000$ W/cm^2 are used in EIT experiments [32].

We would like to emphasize that other applications based upon nonlinear effects might have different and less restrictive requirements on the peak intensity or power of the probe pulse. As a low loss medium with enhanced nonlinearity [33], with small spot size due to small condensate cross section, self-focusing effects and EIT on the probe beam focusing, many nonlinear effects of various interest could be realized with low powers in the condensates in the EIT configuration. Our focus and the purpose here is to examine the standard method of dispersion compensation via nonlinearity so that number of pulses that can be simultaneously present in the condensate can be optimized more directly. In the earlier sections, we have discussed indirect methods based upon adjusting control field intensity as well as taking advantage of higher dimensional pulse propagation and the transverse optical modes inside the condensate to enhance the optical storage capacity. The present section demonstrates the possibility of exploiting nonlinear compensation. With less demanding probe pulse power requirements, rich physical situations can be created such as quantum correlations in the weak probe induced by the nonlinearity [25]. From classical point of view the relatively simpler theory of nonlinear pulse propagation is employed here. Beyond dispersion compensation, such a simple and well developed theory can also lead to rich applications and some novel effects, in particular in the context of dark and bright ultraslow soliton propagation [27,28,29], coupled matter wave and optical field nonlinear dynamics, and so on. However their discussion is beyond the scope of the present paper, which is limited to optical storage capacity enhancement in BECs.

4 Conclusion

We have investigated the problem of injecting multiple ultraslow pulses through a BEC. We have examined three methods for that aim. This paper first reviews our two earlier results where nonlinear optical response is ignored, then also presents our new results where nonlinearity is present. In our first study, we have considered short ultraslow pulse propagation in one dimension. Taking into account group velocity dispersion, an optimum set of experimental parameters, in particular Rabi frequency of control field, that would give maximum pulse storage capacity are determined. Secondly, transverse direction is taken into consideration, and waveguiding of ultraslow pulses is studied. Existence of ultraslow transverse modes is revealed and their benefits in enhancement of pulse storage capacity is pointed out. Finally, in our new results, we have introduced nonlinear optical response and showed that it is possible to compensate dispersion of a short ultraslow pulse for a specifically chosen peak power of the pulse. This may be more efficient in optical storage than group velocity dispersion by the Rabi frequency of the control field. We hope these studies complement ongoing experimental efforts for practical storage of coherent optical information in atomic Bose-Einstein condensates.

5 Acknowledgements

O.E.M. gratefully acknowledges support from a TÜBA/GEBİP grant. We thank N. Postacioglu for many fruitful discussions and for help in numerical computations.

References

1. M. H. Anderson *et. al.*, Science **269**, 198 (1995); C. C. Bradley *et. al.*, Phys. Rev. Lett. **75**, 1687 (1995); K. B. Davis *et. al.*, Phys. Rev. Lett., **75**, 3969 (1995).
2. L.V. Hau, S.E. Harris, Z. Dutton, and C.H. Behroozi, Nature **397,** 594-598 (1999).
3. S. E. Harris, Physics Today **50,** 36-42 (1997).
4. J. P. Marangos, J. Mod. Opt. **45,** 471-503 (1998).
5. C. Liu, Z. Dutton, C. H. Behroozi, and L. V. Hau, Nature **409,** 490-493 (2001).
6. Z. Dutton and L. V. Hau, Phys. Rev. A **70** 053831 (2004).
7. N. S. Ginsberg, S. R. Garner, and L. V. Hau, Nature **445**, 623 (2007).
8. D. Tarhan, A. Sennaroglu, and Ö. Müstecaplıoğlu, Journal of Optical Society of America B **23(9),** 1925-1933 (2006).
9. D. Tarhan, N. Postacioglu, and Ö. Müstecaplıoğlu, Optics Lett. **32** 1038 (2007).
10. Ö. Müstecaplıoğlu and L. You, Optics Commun. **193**, 301 (2001).
11. Ö. Müstecaplıoğlu and L. You, Phys. Rev. A **64**, 013604 (2001).
12. G. Morigi and G. Agarwal, Phys. Rev. A **62**, 013801 (2000).
13. G.S. Agarwal and S. Das Gupta, Phys. Rev. A 65, 053811, 1-5, 2002.
14. X.-G. Wei, J.-H. Wu, G.-X. Sun, Z. Shao, Z.-H. Kang, Y. Jiang, and J.-Y. Gao, Phys. Rev. A **72,** 023806 (2005).

15. V. A. Sautenkov, Y. V. Rostovtsev, C. Y. Ye, G. R. Welch, O. Kocharovskaya, and M. O. Scully, Phys. Rev. A **71,** 063804 (2005).
16. Q. Sun, Y. V. Rostovtsev, J. P. Dowling, M. O. Scully, and M. S. Zubairy, Phys. Rev. A **72,** 031802(R) (2005).
17. M. Bashkansky, G. Beadie, Z. Dutton, F. K. Fatemi, J. Reintjes, and M. Steiner, Phys. Rev. A **72,** 033819 (2005).
18. S.E. Harris, J.E. Field, and A. Kasapi, Phys. Rev. A **46**, R29 (1992).
19. M. Naraschewski, D. M. Stamper-Kurn, Phys. Rev. A **58,** 2423-2426 (1998).
20. L.-M. Duan, J.I. Cirac, and P. Zoller, Phys. Rev. A **66,** 023818 (2002).
21. A. André, M. Bajcsy, A.S. Zibrov, and M.D. Lukin, Phys. Rev. Lett. **94**, 063902 (2005).
22. J. Cheng, S. Han, and Y. Yan, Phys. Rev. A **72**, 021801(R) (2005).
23. M. Vengalattore and M. Prentiss, Phys. Rev. Lett. **95**, 243601 (2005).
24. Z. Dutton, M. Budde, C. Slowe, L. V. Hau, Science **293,** 663-668 (2001).
25. I. Vadeiko, A. V. Prokhorov, and S. M. Arakelyan Phys. Rev. A **72,** 013804 (2005).
26. G. P. Agrawal, *Nonlinear Fiber Optics*, (Academic Press,San Diego, California 1995), pp.101.
27. A.V. Rybin, I. P. Vadeiko, A. R. Bishop, Phys. Rev. E. **72**, 026613 (2005).
28. Y. Wu and L. Deng, Optics Lett. **29**, 2064-2066 (2004).
29. G. Fanjoux, J. Michaud, H. Maillotte, and T. Sylvestre, Phys. Rev. Lett. **100** 013908 (2008).
30. S. wielandy and A. L. Gaeta, Phys. Rev. A **58**, 2500-2505 (1998).
31. J. Zhang, G. Hernandez, and Y. Zhu, Optics Lett. **33**, 46-48 (2008).
32. M. M. Kash, V. A. Sautenkov, A. S. Zibrov, L. Hollberg, G. R. Welch, M. D. Lukin, Y. Rostovtsev, E. S. Fry, and M. O. Scully, Phys. Rev. Lett. **82**, 5229-5232 (1999).
33. H. Wang, D. Goorskev, and M. Xiao, Phys. Rev. Lett. **87**, 073601 (2001).